Energy and Buildings 127 (2016) 648–657

Contents lists available at ScienceDirect

Energy and Buildings

journal homepage: www.elsevier.com/locate/enbuild

Effect of supply/exhaust diffuser configurations on the contaminant distribution in ultra clean environments: Eulerian and Lagrangian approaches

Jaber Eslami [a], Abbas Abbassi [a,*], Mohammad H. Saidi [b], Majid Bahrami [c]

[a] Mechanical Engineering Department, Amirkabir University of Technology, 424 Hafez Ave., P.O. Box 15916-34311, Tehran, Iran
[b] Center of Excellence in Energy Conversion (CEEC), School of Mechanical Engineering, Sharif University of Technology, Tehran, Iran
[c] Mechatronic Systems Engineering Department, Simon Fraser University, Surrey, Canada

ARTICLE INFO

Article history:
Received 30 July 2015
Received in revised form 8 June 2016
Accepted 9 June 2016
Available online 11 June 2016

Keywords:
Cleanroom
Eulerian approach
Lagrangian approach
Particle
Supply/exhaust configurations

ABSTRACT

In this research, the airflow pattern and particle dispersion in a contaminated full-scale cleanroom are investigated numerically using both Eulerian and Lagrangian approaches. Three different supply diffuser configurations namely (1) central, (2) horizontal and (3) vertical and three different exhaust grille configurations namely (4) vertical symmetric, (5) asymmetric and (6) horizontal symmetric are selected for the analysis. The presented results reveal that the supply/exhaust openings arrangement has a significant influence on the particulate contaminant dispersion in the cleanrooms. The comparison of the above different supply diffuser configurations shows that the vertical and horizontal supply diffuser configurations lead to a more escaped particles and less deposited particles on the room walls and installed working table in the room than the central one. It is also found that for different exhaust grille arrangements, the performance of the ventilation system in the horizontal symmetric case is higher than asymmetric and vertical symmetric ones. At the same time, it is observed that the variations of contaminant concentration in both Eulerian and Lagrangian approaches are almost the same. The results of the velocity and particle concentration show good agreement with the available experimental data in the literature.

1. Introduction

Indoor air quality (IAQ) is crucial for both human health and manufacturing processes. In many industries such as pharmaceutical, food processing, biotech, aerospace, optics, microelectronics and operating rooms, particulate contamination has a significant effect on IAQ. In recent decades, cleanrooms have been extensively used to decrease particulate contamination, as well as to control other environmental parameters such as temperature, humidity and pressure to provide an appropriate comfort level [1,2]. Better dilution of dispersed contaminant from cleanrooms is a fundamental factor for the cleanroom ventilation system design. The dispersion of the contaminant directly depends on the type of airborne particles and the airflow pattern within the cleanrooms. The airborne particles are transported with a large volume of air that enters from supply diffusers and away from critical zones such as working table. The airflow pattern and the turbulence can be the most efficacious factor on particle transportation [3]. Therefore, based on the cleanroom flow field, the investigation of airborne contaminant concentration and developing a new method to reduce this effect is essential.

Since the 90s, with significant improvement in the computational capacity, computational fluid dynamics (CFD) has become a powerful and efficient tool to study engineering problems including airflow and airborne contaminant distribution in enclosures. It is known that there are two main particle transport approaches in CFD simulations: (1) the Eulerian-Eulerian (E-E), and (2) the Eulerian-Lagrangian (E-L) approach. Considering computational cost, the E-L approach is more suitable for particle concentration modeling for transient state whereas for steady state, the E-E approach simulates concentration in less computational time than E-L approach [4]. Several investigations have been made to explore the effect of different factors that influence the contaminant concentration in cleanrooms with two aforementioned approaches. The main factors such as airflow pattern, particle characteristics, the location of obstacles [5], contaminant source location [4–6], supply/exhaust openings arrangement [7–9] are reported in the literature.

* Corresponding author.
E-mail addresses: abbassi@aut.ac.ir, abbassi3410@gmail.com (A. Abbassi).

http://dx.doi.org/10.1016/j.enbuild.2016.06.028
0378-7788/

Nomenclature

Abbreviations

CFD	Computational fluid dynamics
DRW	Discrete random walk
E-E	Eulerian-Eulerian
E-L	Eulerian-Lagrangian
IAQ	Indoor air quality
RANS	Reynolds averaged Navier–Stokes
RNG	Renormalization group
UDF	User defined function

Greek symbols

ε	Energy dissipation rate
ρ	Density of the fluid
ρ_p	Density of the particle
μ_{eff}	Air effective viscosity
μ_l	Laminar viscosity
μ_t	Turbulent viscosity
τ	Particle relaxation time
τ^*	Dimensionless time
τ_c	Particle eddy crossing time
τ_e	Lifetime of the turbulent energy
λ	Mean free path
η	Ratio of turbulent to mean strain time scale
$\sigma_k, \sigma_\varepsilon$	Model constants in the RNG k-ε model
β	Volumetric expansion coefficient

Subscripts

i, j	Spatial coordinates
in	Inlet
L	Lagrangian
P	Particle

Latin symbols

A_{in}	Inlet area
C_c	Cunningham slip correction factor
$C_{1\varepsilon}, C_{2\varepsilon}$	Model constants in the RNG k-ε model
C_μ	Model constant in the RNG k-ε model
c	Contaminant concentration
c_j	Mean particle concentration in a cell
D	Molecular diffusion rate
d_p	Particle diameter
$dt_{(i,j)}$	Particle residence time
F_a	Additional forces
G	Gaussian random number
g_i	Gravitational constant in i direction
k	Turbulent kinetic energy
Kn	Knudsen number
L_e	Eddy length scale
$\dot{M}$	Flow rate
P	Turbulent energy production rate
p	Pressure
S	Particle to fluid density ratio
Sc_t	Schmidt number
T_L	Turbulent lagrangian time scale
t	Time
U_{in}	Inlet velocity
u_i	Fluid mean velocity components
u_i^p	Particles velocity components
u_i'	Turbulent fluctuating velocity components
V	Cleanroom volume
V_j	Volume of a computational cell
x, y, z	Rectilinear orthogonal coordinates

One of the main parameters which may impact the contaminant concentration, especially in ultra-clean environments, is the configurations of supply and exhaust diffusers [10]. Zhao et al. [11] numerically studied the aerosol particle concentration and deposition in displacement and mixing ventilation rooms. Their results showed that a displacement-ventilated room had a lower particle deposition rate and larger escaped particle mass than the mixing one, while the average particle concentration of displacement case was higher than the mixing case. Sadrizadeh et al. [12] investigated the effectiveness of vertical and horizontal ventilation system on the particle distribution in the surgical zone. They found that the preferred selection between vertical and horizontal ventilation scenario in an operating room was highly dependent on internal constellation of obstacles, work practice, and the supply airflow rate.

Although, some researchers have studied the particle movement, deposition and distribution in indoor airflow, few investigations have been found in the literature to explore the effectiveness of different supply/exhaust configurations in reducing contaminant in the cleanroom.

In the present paper, the effect of supply diffuser and exhaust grille configurations on the contaminant transport in cleanrooms is studied numerically using both E-E and E-L approaches. To compare the contaminant distribution, particles are supposed to be uniformly distributed in the model cleanroom and the ventilation system removes contaminant from the model room. The following questions will be investigated:

1) What is the effect of different supply/exhaust opening arrangements on the contaminant distribution in a model cleanroom?
2) Which configuration has better effectiveness to discharge contaminant from the cleanroom? Is there any significant difference between the percentages of escaped and deposited particles for different configurations?
3) Is there difference between E-E and E-L approaches to predict the contaminant concentration distribution for a model cleanroom?

The goal of this study is to provide detailed knowledge and engineering guidelines for better design in future cleanrooms.

2. Analysis of numerical method

This investigation compares the two modeling approaches with an emphasis on their performance of predicting particle concentration distributions in ventilated spaces. Both the E-E and E-L models under examination are performed based on the same airflow field calculated by solving the Reynolds Averaged Navier–Stokes (RANS) equations with the Renormalization Group (RNG) $k-\varepsilon$ turbulence model.

2.1. Flow model

2.1.1. Governing equations

As the contaminant concentration in cleanrooms is very low, the airflow hydrodynamics is not affected by the contaminant phase. Therefore the interaction between continuous airflow phase and particle discrete phase are treated as one-way coupling [4]. Considering Boussinesq's turbulent viscosity hypothesis [13], the flow governing equations are as follows [14]:

Continuity equation:

$$u_{i,i} = 0 \tag{1}$$

where u_i are the mean velocity components.

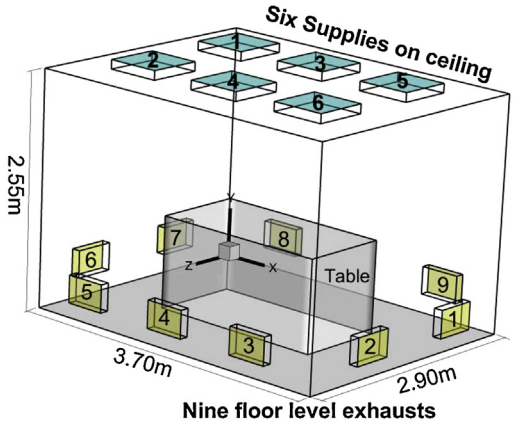

Fig. 1. Schematic of the investigated cleanroom model available in Sharif University of Technology, Cleanroom Research Laboratory.

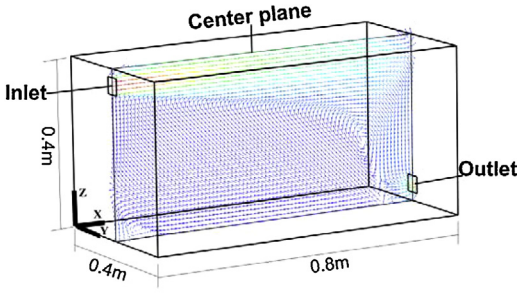

Fig. 2. Schematic of the validation model room.

Momentum equations:

$$u_j u_{i,j} = -\frac{1}{\rho} p_{,i} + \frac{\mu_{eff}}{\rho}(u_{i,j} + u_{j,i})_{,j} \tag{2}$$

where μ_{eff} is the air effective viscosity.

$$\mu_{eff} = \mu_l + \mu_t \tag{3}$$

here μ_l and μ_t are the laminar and the turbulent viscosities, respectively.

To resolve the turbulence closure problem, an RNG $k-\varepsilon$ model [15] is used in this study to predict the turbulent viscosity.

$$\mu_t = C_\mu \rho \frac{k^2}{\varepsilon} \tag{4}$$

where $C_\mu = 0.0845$, and k and ε are the turbulent kinetic energy and the energy dissipation rate, respectively. The governing equations for k and ε are:

$$\rho\frac{\partial k}{\partial t} + \rho\frac{\partial (k u_i)}{\partial x_i} = \frac{\partial}{\partial x_j}\left[\left(\mu + \frac{\mu_t}{\sigma_k}\right)\frac{\partial k}{\partial x_j}\right] + G - \rho\varepsilon \tag{5}$$

$$\rho\frac{\partial \varepsilon}{\partial t} + \rho\frac{\partial (\varepsilon u_i)}{\partial x_i} = \frac{\partial}{\partial x_j}\left[\left(\mu + \frac{\mu_t}{\sigma_\varepsilon}\right)\frac{\partial \varepsilon}{\partial x_j}\right] + C_{1\varepsilon}\frac{\varepsilon}{k}G - C^*_{2\varepsilon}\rho\frac{\varepsilon^2}{k} \tag{6}$$

$$C^*_{2\varepsilon} = C_{2\varepsilon} + C_\mu \frac{\eta^3\left(1-\eta/\eta_0\right)}{1+\beta\eta^3} \tag{7}$$

where G is the turbulent energy production rate, $\eta = \left(Sk/\varepsilon\right)$ with $S = \sqrt{2S_{ij}S_{ij}}$ and $C_{1\varepsilon} = 1.42$, $C_{2\varepsilon} = 1.68$, $\sigma_k = 0.7194$, $\sigma_\varepsilon = 0.7194$, $\beta = 0.012$, $\eta_0 = 4.38$ are taken from Yakhot et al. [16].

2.2. Particle phase modeling

Generally, there are two approaches of modeling particle concentration in CFD simulations: (1) the Eulerian method, and 92) the Lagrangian method [4]. In the present work, to investigate the effects of supply/exhaust openings arrangement on the contaminant dispersion, both E-E and E-L approaches are used to simulate contaminant concentration. Both methods use the same Eulerian model for airflow, but the E-E method, considers the particle phase as a continuum whereas the E-L method, tracks all particle trajectories in the room for discrete phase modeling.

2.2.1. The Eulerian approach

The E-E model solves one conservation equation for particulate phase. In this study, similar to the literature [4,14] the type of Eulerian method is single fluid model. This model takes into account the contaminant phase as a modified scalar, as such the particle concentration take the following [4]:

$$\frac{\partial c}{\partial t} + u_i c_{,i} = \left[D + \frac{\mu_t}{\rho Sc_t}\right] c_{,ii} \tag{8}$$

where c is the contaminant concentration and D is the molecular diffusion rate of particle and Sc_t turbulence Schmidt number. For

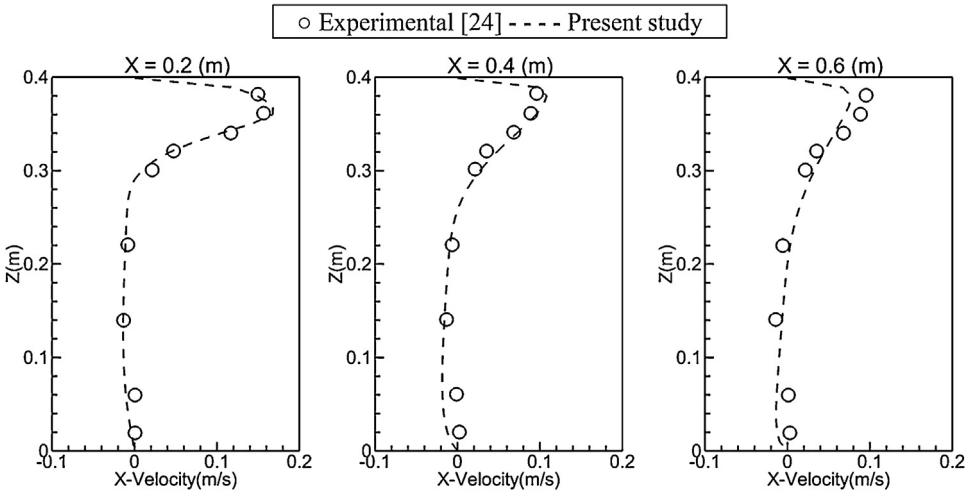

Fig. 3. Comparison of Chen et al.'s measured data [24] and predicted x-velocity at three different locations.

Table 1
Specifications of six cases of supply/exhaust configurations for air change rate of 60.0 and supply diffusers velocity of 0.63 (m/s).

Case name	Case configuration	Active exhaust grilles	Active supply diffusers
Case 1	Central	1–5	3,4
Case 2	Horizontal	1–5	1,5
Case 3	Vertical	1–5	1,2
Case 4	Vertical symmetric	1,2,6,7	3,4
Case 5	Asymmetric	1,2,3,5	3,4
Case 6	Horizontal symmetric	3,5,8,9	3,4

coarse particles in a turbulent flow the molecular diffusion rate of particle will be negligible compared with the turbulent term.

2.2.2. The Lagrangian approach

For E-L particle tracking and to calculate trajectory of discrete phase particle, the particle motion equation becomes [17]:

$$\frac{du_i^p}{dt} = \frac{1}{\tau}\left(u_i - u_i^p\right) + \frac{g_i\left(\rho_p - \rho\right)}{\rho_p} + F_a \tag{9}$$

where u_i and u_i^p are the fluid and the particles velocities, ρ and ρ_p are the density of the fluid and the particles, g_i and F_a are the gravity and additional forces, respectively. In this research, based on the literature [17,11] additional forces, such as Saffman lift force caused by shear, virtual mass force [17], thermophoretic force [17], Brownian force [17], Basset force [17] and pressure gradient force [17] are assumed negligible due to relatively large size of the investigated particles. The particle relaxation time τ is defined as [17]:

$$\tau = \frac{Sd_p^2 C_c}{18\nu} \tag{10}$$

where d_p is the particle diameter, S is the particle to fluid density ratio and Cunningham slip correction factor C_c [17] is implemented to compensate non-continuum effects:

$$C_c = 1 + 2Kn\left[1.257 + 0.4exp\left(\frac{-1.1}{2Kn}\right)\right] \tag{11}$$

where Knudsen number is defined as:

$$Kn = \frac{2\lambda}{d_p} \tag{12}$$

In Eq. (12), λ is the air mean free path, which equals to 68 nm in the normal conditions (T = 25 °C and P = 1 atm). As the turbulence diffusion is one of the most important features of the indoor airflow, its accurate estimation is necessary to predict the particle trajectory. In this study, the Lagrangian discrete random walk (DRW) model is used following [17], in which the turbulent fluctuating velocity components are simulated as:

$$u_i' = G\sqrt{u_i'^2} \tag{13}$$

where G is a Gaussian random number and $\sqrt{u_i'^2}$ is the root mean square (RMS) of the fluctuating velocity components. For the $k-\varepsilon$ family turbulence models, the RMS components are identical and equal to $2k/3$.

To evaluate the appropriate time to update the random number$G$, eddy lifetime and particle crossing time concepts are used. The characteristic lifetime of the turbulent energy containing eddies is assumed to be constant and is defined as:

$$\tau_e = 2T_L \tag{14}$$

where T_L is the turbulent Lagrangian time scale and for $k-\varepsilon$ family turbulence models can be estimated as:

$$T_L = 0.15\frac{k}{\varepsilon} \tag{15}$$

The particle eddy crossing time which is the time a particle needs to pass across an eddy, is defined as:

$$\tau_c = -\tau\left[1 - \frac{L_e}{\tau|u - u_p|}\right] \tag{16}$$

where L_e is the eddy length scale and for $k-\varepsilon$ turbulence models can be approximated as:

$$L_e = 0.16\frac{k^{3/2}}{\varepsilon} \tag{17}$$

The particle is assumed to interact with the eddies over the smaller value of τ_e and τ_c [17]; so the random number G should be updated at this time.

To compare E-E and E-L approaches, it is necessary to show particle trajectory as concentration form. So the particle source in cell (PSI-C) method [18] can be used as:

$$c_j = \frac{\dot{M}\sum_{i=1}^{m} dt_{(i,j)}}{V_j} \tag{18}$$

where c_j is the mean particle concentration in a cell and $\dot{M}$ is the flow rate of each trajectory, $dt_{(i,j)}$ is the particle residence time at the ith trajectory and the jth cell, and V_j is the volume of a computational cell for particles.

For a convenient definition of a time of the solution, a new dimensionless time is introduced in Eq. (19):

$$\tau^* = \frac{t}{V/A_{in}U_{in}} \tag{19}$$

Table 3
Statistical analysis of the error in normalized concentration at three different locations.

	X = 0.2 m		X = 0.4 m		X = 0.6 m	
	E-L	E-E	E-L	E-E	E-L	E-E
Mean relative error (%)	21	22	16	15	12	18
Standard deviation (%)	23	16	6	10	8	10
Standard error	8	5	2	3	3	3

Table 4
Summary of normalized concentration for the three cases for the elapsed time of 100.0 s at the plane Y = 1.1 m.

	Case 1		Case 2		Case 3	
	E-E	E-L	E-E	E-L	E-E	E-L
Mean	0.07	0.04	0.05	0.03	0.04	0.02
Maximum	0.20	0.18	0.20	0.23	0.11	0.15
Minimum	0	0	0	0	0	0
Standard deviation	0.04	0.04	0.05	0.04	0.03	0.03

Table 2
Boundary conditions for simulation.

Name	Boundary type	Velocity	Lagrangian model	Eulerian model
Room walls (sidewalls, ceiling, working table)	Wall	No slip	Trap	Concentration: 0
Supply	Velocity inlet	0.63 m/s	Escape	Concentration: 0
Exhaust	Pressure outlet	–	Escape	Concentration flux: 0
Floor	Wall	No slip	Trap	Deposition particle mass flux

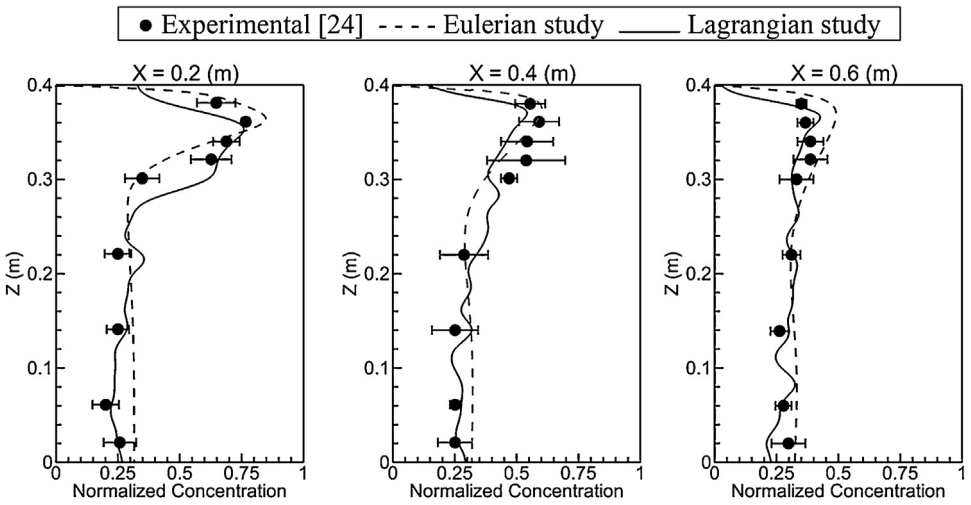

Fig. 4. Comparison of Chen et al.'s measured data [24] and predicted normalized concentrations at three different locations.

Table 5
Comparison of the percentage of escaped, deposited and suspended particles with and without E-L DRW model for the three cases for the elapsed time of 130.0 s.

	Case 1		Case 2		Case 3	
	Without DRW	With DRW	Without DRW	With DRW	Without DRW	With DRW
Escaped (%)	75	46	73	48	75	50
Deposited (%)	15	53	22	51	21	49
Suspended (%)	10	1	5	1	4	1

where V, A_{in} and U_{in} are the cleanroom volume, inlet area and velocity, respectively.

2.3. Boundary and initial conditions

In this study, velocity inlet and pressure outlet boundary conditions are used for supply diffusers and exhaust grilles, respectively. Considering an air change rate (ACH) of 60/h, a uniform and constant supply diffusers velocity of 0.63 m/s with 5% turbulence intensity is used. All boundary walls are supposed to be adiabatic and the no-slip condition is used for the velocity at the walls. It is also assumed that the contaminant is initially uniformly distributed in the model room and the ventilation system removes the contaminant. In the E-L approach, the trajectories of particles are vanished when they impact the walls of the cleanroom or the working table and the particles leave the cleanroom from exhaust grilles. In the E-E approach, zero concentration is used for sidewalls and ceiling. For the floor boundary condition, according to the same study [19], a user defined function (UDF) is used to calculate the deposition particle mass flux based on the model of Lai et al. [20]. Also, the zero flux concentration is considered for the boundary condition on exhausts. These boundary conditions for the simulation are listed in Table 2.

2.4. Solution procedure

In this study a second-order upwind scheme is used for discretizing and a SIMPLE algorithm is adapted for coupling between pressure and velocity [21]. As the RNG $k-\varepsilon$ model, mentioned above, fails in the near wall region, the standard wall function is implemented to extract the airflow turbulent properties in this zone, more details are given by Launder and Spalding [13]. ICEM CFD ANSYS software [22] is used to mesh a cleanroom. The mesh type is structured hexahedral and the grid independency test is conducted using three different mesh densities of 205000, 420000 and 600000 cells. Based on insignificant difference between 420000 and 600000 cells, it makes sure that a mesh density of 420000 cells is fine enough to predict the velocity, turbulence and concentration in the domain. Airflow pattern and concentration field are modeled numerically based on the finite volume method (FVM) and a commercial software ANSYS FLUENT 15.0 [23] is used.

3. Validation of the numerical method

To validate the present study, the x-direction velocity in a three-dimensional model room is investigated numerically and compared against experimental data from Chen et al. [24]. Dimensions of the model room under study is L(X) × H(Y) × W (Z) = 0.8m × 0.4m × 0.4m. The fresh air enters the room through the inlet H(Y) × W (Z) = 0.04m × 0.04 m that is located on the centerline of the room and symmetrically exhausted from the outlet H(Y) × W (Z) = 0.04m × 0.04 m in the faced side, as shown in Fig. 2. The air change per hour (ACH) used for the experiment was 10/h, accordingly, the inlet velocity was 0.225 m/s. RNG $k-\varepsilon$ turbulent model is utilized to simulate x-velocity at three different locations namely x = 0.2m, x = 0.4 m and x = 0.6 m corresponding to experimental data [24]. The numerical x-velocity is in good agreement with the experimental data [24], as shown in Fig. 3. For the validation of the contaminant concentration in the E-E model, the inlet concentration and the initial concentration of the room is specified as 1 and 0, respectively. On the other side, for the E-L DRW model, 60,000 tracking particles with 10 μm diameter and a density of 1400 kg/m^3 are injected through the inlet. Fig. 4 demonstrates the comparisons of predicted normalized concentration by both E-E and E-L approaches against experimental data from Chen et al. [24]. Furthermore, Table 3 shows the statistical analysis of the error in normalized concentration by using these two approaches at three different locations. As shown in Fig. 4 and Table 3, the comparison of the normalized concentration in both E-L and E-E approaches exhibits a fairly good agreement with a maximum mean relative error of 21% and 22%, respectively.

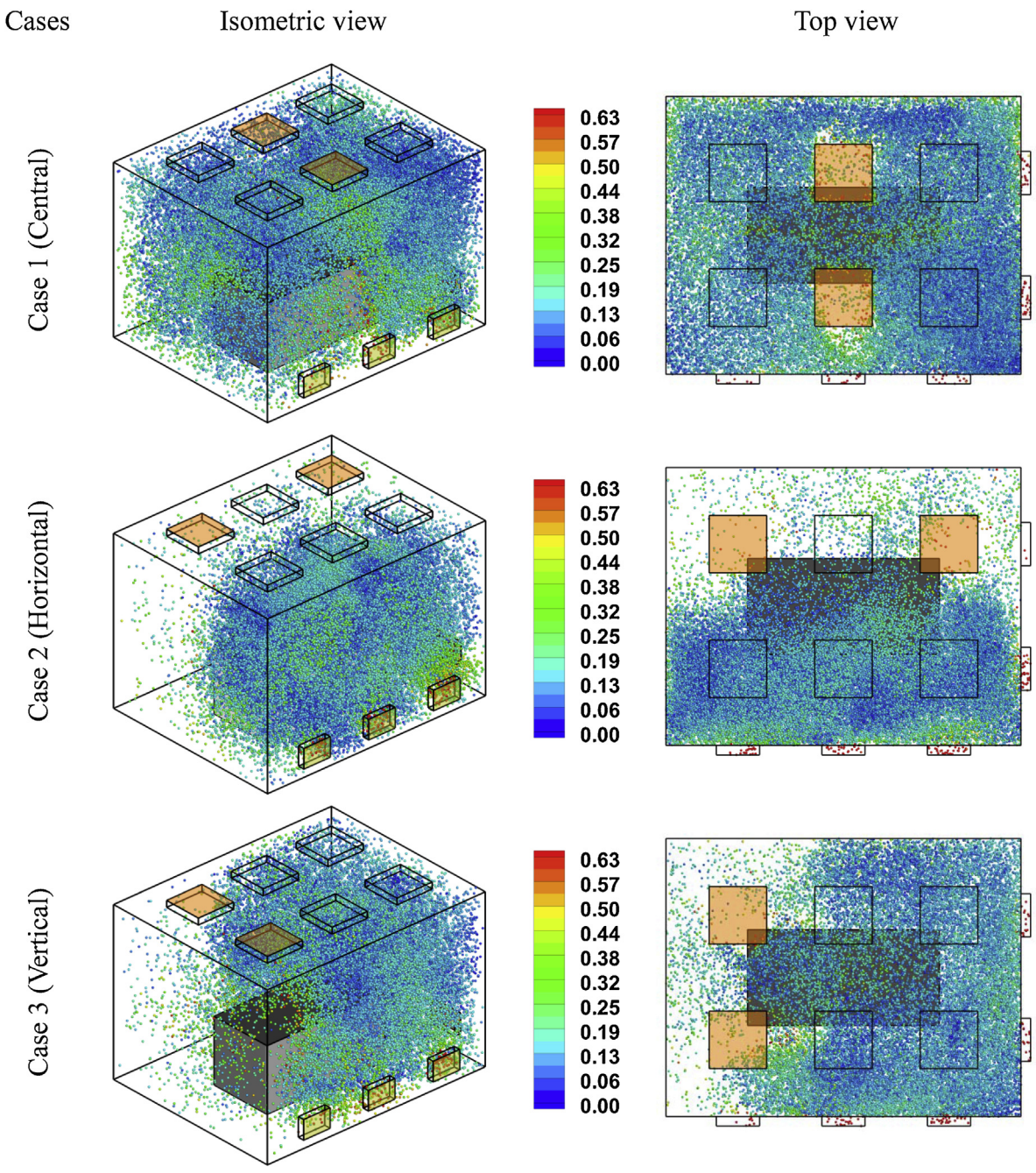

Fig. 5. Isometric view and top view of particles dispersion through the enclosure for the three cases for elapsed times are 100.0s.

4. Case study

In this study, to compare the performance of ventilation system to discharge of contaminant, six different supply/exhaust air diffuser configurations with two modeling approaches are selected and studied. As shown in Fig. 1, the geometry of the simulated cleanroom is set the same as the full-scale test room available in the Sharif University of Technology, Cleanroom Research Laboratory in which we call it model room in this study.

The dimensions of the model room are L(X) × W (Z) × H(Y) = 3.7m × 2.9m × 2.55m. The model room is ventilated with two standard L(X) × W (Z) = 0.6 m × 0.6 m supply diffusers, located at the ceiling level. Nine W (Z) × H(Y) = 0.45m × 0.3 m exhaust grilles, spaced on the cross vertical wall, exhaust the air flow to return air channel. A flat working table is also considered in the middle of this cleanroom with the dimensions of L(X) × W (Z) × H(Y) = 2m × 1m × 1m. Six supply/exhaust air diffuser configurations namely (1) central, (2) vertical, (3) horizontal, (4) vertical symmetric, (5) horizontal symmetric and (6) asymmetric are investigated as presented in Table 1.

5. Results and discussion

In the present work, for the means of comparison, the steady flow fields of both E-E and E-L approaches are the same. For E-E contaminant distribution modeling, the initial concentration of contaminated room is specified as 1. The E-L approach tracks transiently a large amount of particles. The method starts from solving the transient momentum equation for each particle. Here, 1,243,577 single sized particles with a mean diameter of 5 μm

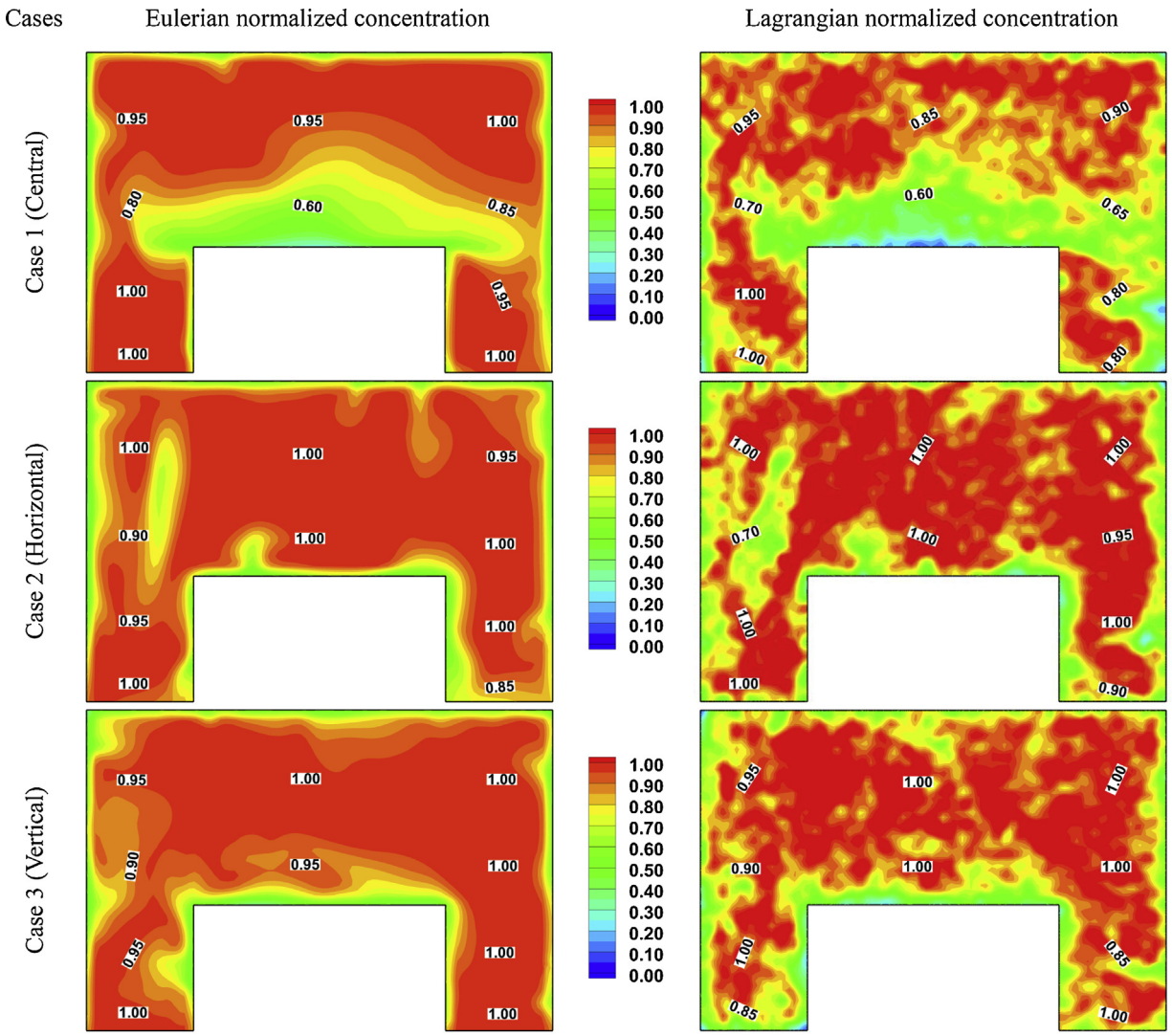

Fig. 6. A comparison of normalized concentration between E-E and E-L approaches for the three cases for the elapsed time of 5.0 s at plane Z = 1.45 m.

and a density of 1000 kg/m^3 were used for the start up of all cases. Obviously, the E-L approach requires considerably more computing time if more particles are tracked [4]. The Lagrangian particle tracking method could introduce uncertainty into particle concentration calculations. This problem is solved under unsteady state conditions for 130 s until all particles are removed from the cleanroom, in other words, the normalized concentration in the cleanroom becomes zero.

Fig. 5 shows the isometric view and top view of particles dispersion in the model room for 100s. The following can be concluded from Fig. 5:

- Different airflow patterns induced by various supply diffuser configurations have an important impact on leading the particles toward the exhaust grilles.
- In the vertical and horizontal configurations, contaminant displaces to one side of the model room. In these cases, supply ventilation airflow pushes the indoor air towards the exhausts, which leads to a better ventilation.
- In the central configuration, contaminant spreads on both sides of the supply diffusers in the whole room. In these cases over mixing effect of the resultant airflow leads to less ventilation effectiveness for discharge of contaminant.
- Considering aforementioned pattern of contaminant movement, it is expected that in the central case, more particles hit the sidewalls of the room and in vertical and horizontal cases more contaminants leave the model room from the exhaust grilles (see Fig. 11). In other words, vertical and horizontal configurations present directional ventilation airflow and provide better IAQ.

Figs. 6 and 7 show a contour view of normalized concentration simulated by E-E and E-L approaches for the elapsed time of 5.0 s at plane Z = 1.45 m and the elapsed time of 100.0 s at plane Y = 1.1 m, respectively. The summary statistics of normalized concentration has been provided in Table 4.The following conclusions can be drawn from Figs. 6 and 7 and Table 4:

- The contour results of E-E and E-L approaches are in logical agreement together, although the E-E indicates smoother contour (see Fig. 6).
- There is a significant difference in the contaminant concentration distribution around the working table for different cases. Lower normalized concentration is observed in the vertical and horizontal cases (see Fig. 7).
- The normalized concentration differences between the central and vertical cases by E-E and E-L approaches are 42% and 50%, respectively (see Table 4).

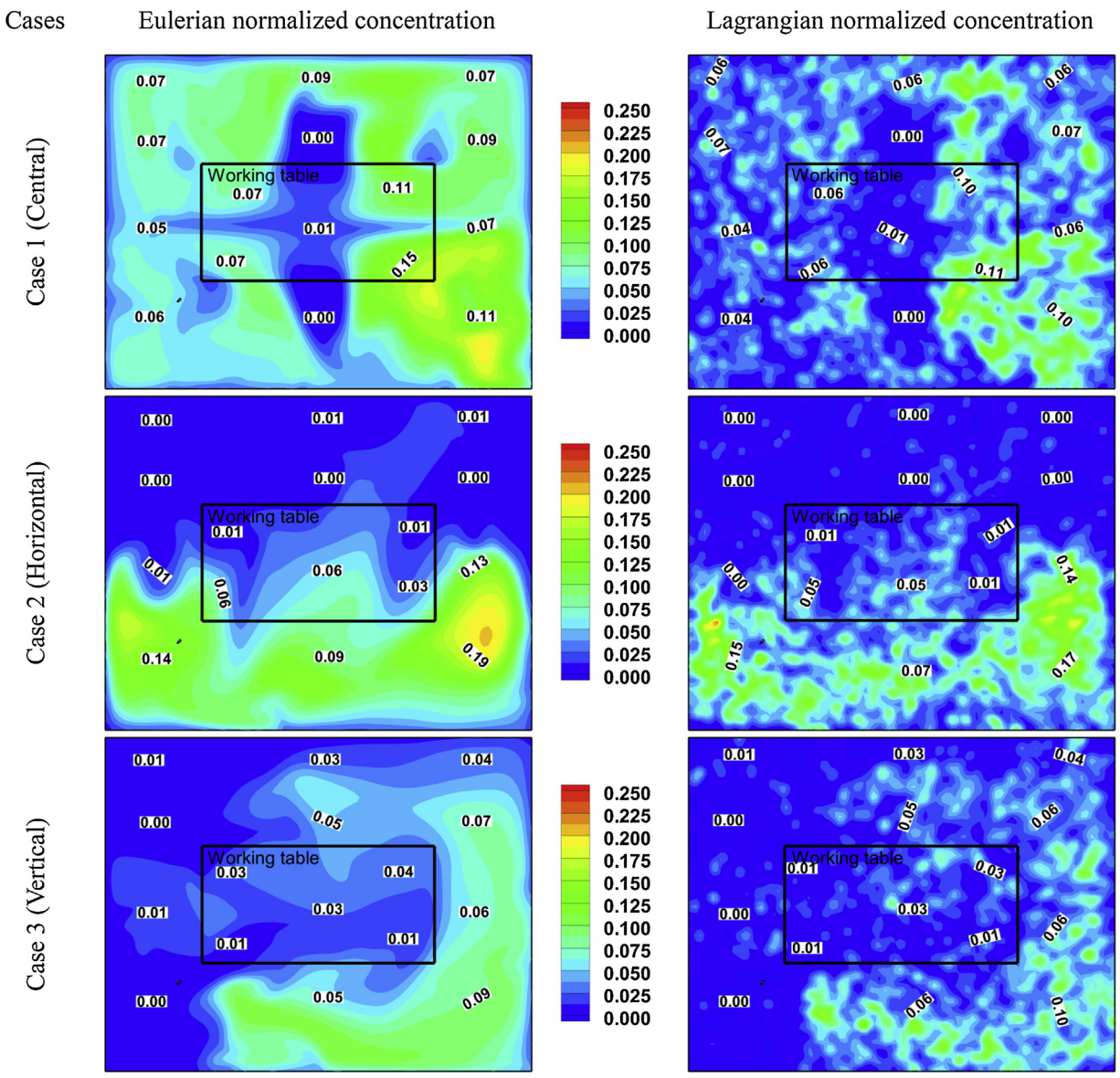

Fig. 7. A comparison of normalized concentration between E-E and E-L approaches for the three cases for the elapsed time of 100.0 s at plane Y = 1.1 m.

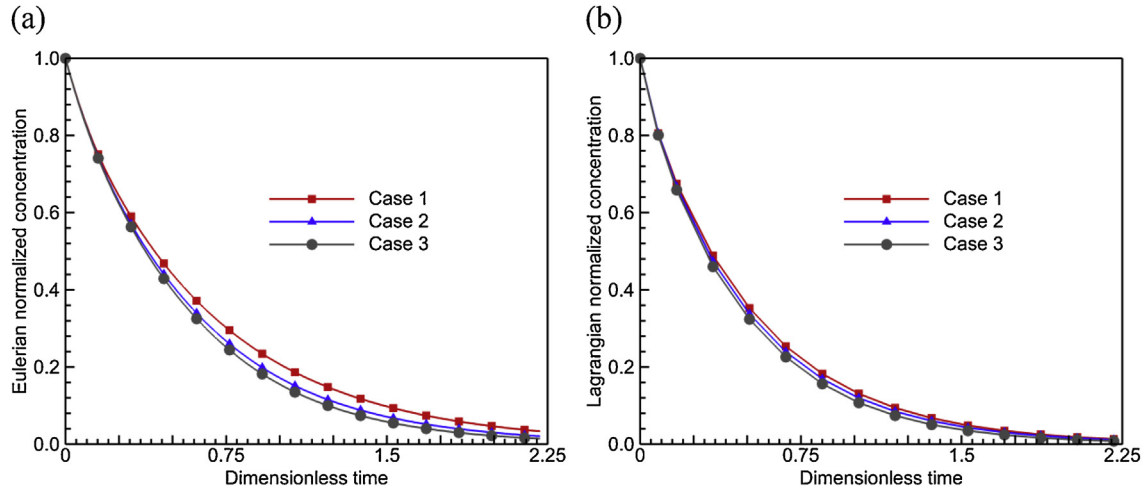

Fig. 8. The normalized concentration for the three cases: (a) E-E, (b) E-L.

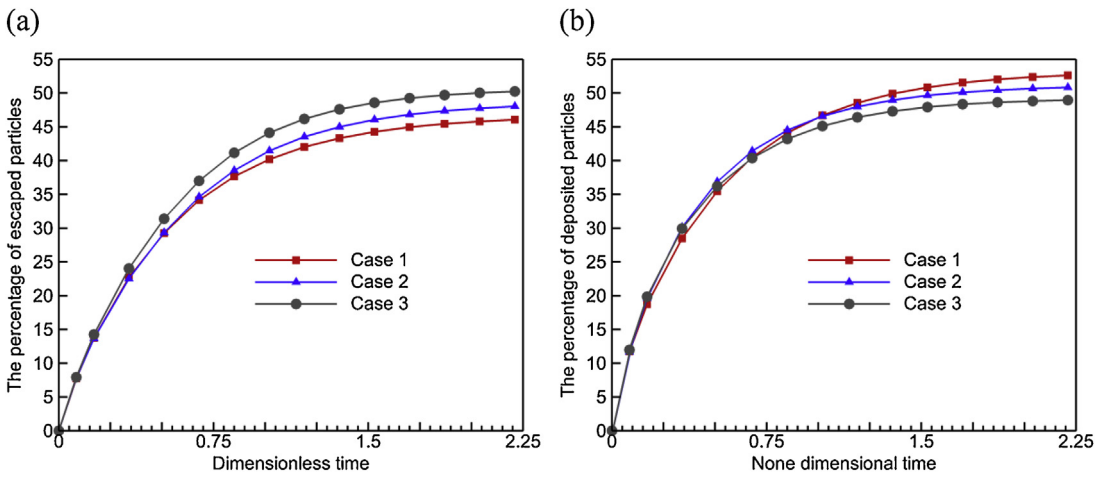

Fig. 9. Comparison of the percentage of particles for the three cases: (a) escaped, (b) deposited.

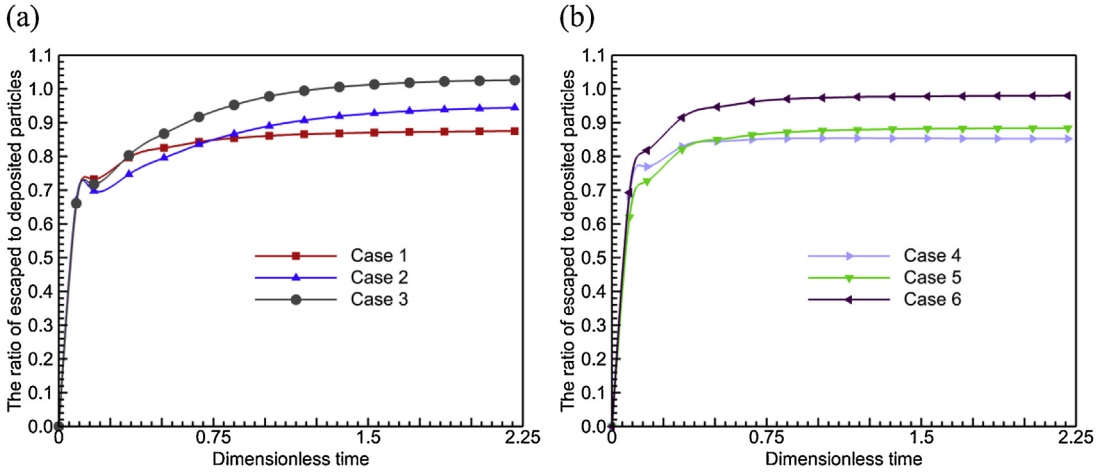

Fig. 10. Comparison of the ratio of escaped to deposited particles for cases: (a) 1–3, (b) 4–6.

Fig. 8 shows the transient variation of normalized concentration in E-E and E-L approaches. The following conclusions can be drawn from Fig. 8:

- The variations of normalized concentration in both E-E and E-L approaches are almost the same.
- In spite of some differences in the final contaminant in the room, which is mainly due to gravitational sedimentation and random behavior in the E-L DRW solution, the overall results are fairly consistent.

Fig. 9 demonstrates the details information about trajectory of particles over the dimensionless time in the E-L approach. It presents more details about trajectory of particles that is important for cleanroom applications, such as the percentage of escaped particles in different exhausts and the percentage of particles that deposit on the room walls and working table. The following highlights the trends in Fig. 9:

- Airflow pattern and turbulence are the main reasons for particles deposition and discharging. When the E-L DRW model is considered, more particle deposition on room walls has been observed that leads to decrease the percentage of escaped particles for all cases. The differences of deposited particles between with and without E-L DRW model are 38% for central case, 29% for horizontal case and 28% for vertical case (see Fig. 9a and Table 5).
- At the end of dilution of room from contaminant, the percentage of escaped particles for horizontal and vertical cases shows ~4.2% difference with central case, while dimensionless time is 2.21 (see Fig. 9a).
- The percentage of deposited particles in central case is ~3.7% more than horizontal and vertical cases (see Fig. 9b).

Due to deposited particles resuspension, the less normalized concentration does not necessarily show the configuration which leads to a better IAQ [11]. In fact, the cases with more escaped and less deposited particles result in a better effectiveness. Furthermore, Fig. 10 depicts the ratio of escaped to deposited particles for different supply/exhaust configurations. The following can be concluded from Fig. 10:

- For different supply diffuser configurations (cases 1–3), the ratio of escaped to deposited particles in the vertical and horizontal cases are higher than central case and yield better IAQ (see Fig. 10a).
- For different exhaust grille arrangements (cases 4–6), difference in the percentage of escaped and deposited particles are observed. The performance of the ventilation system to discharge the contaminant in the horizontal symmetric case is better than asymmetric and vertical symmetric cases. Among these three cases the maximum percentage of deposited (~53%) and escaped

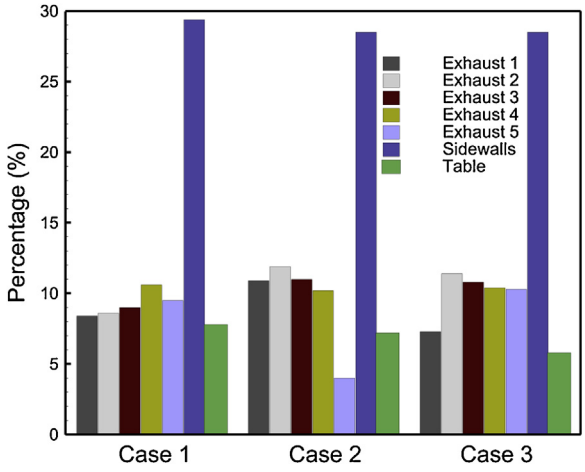

Fig. 11. Comparison of the percentage of the escaped and deposited particles on different boundaries.

(~49%) particles are for vertical symmetric and horizontal symmetric cases, respectively (see Fig. 10b).

Fig. 11 shows the escaped and deposited particles of different boundaries. The following highlights the trends in Fig. 11:

- Most of the particles in the central and vertical cases escape from exhaust 4 and exhaust 2, respectively, although in the vertical case, the total number of escaped particles is more than the central case.
- The percentage of deposited particles on the walls and the working table, rank from most to least: the central, horizontal and vertical ones.
- The most and the least percentages of deposited particles on the working table are for central and vertical cases, respectively with ~34% difference.

6. Conclusions

In this research, the effect of different supply/exhaust openings configurations on the ventilation system effectiveness of cleanroom was studied numerically using both E-E and E-L approaches. Based on the same airflow domains, the comparisons of contaminant concentration for six different cases are performed and the following conclusions can be reached.

(1) The layout of supply/exhaust openings has a great influence on the contaminant dispersion through an enclosure.
(2) Results of both E-E and E-L approaches show that for different supply diffuser arrangements, the ventilation system performance for contaminant dilution is improved using vertical and horizontal layout which provides directional airflow through the enclosure. The vertical and central configurations show the best and the worst performance to remove contamination from this model room, respectively.
(3) For different exhaust grille arrangements, the model ventilation performance in the horizontal symmetric case is better than asymmetric and vertical symmetric cases and yield better IAQ.
(4) The variations of normalized concentration in both E-E and E-L approaches are almost the same.

This study and its results provides a better understanding of the supply/exhaust openings configurations on the indoor air quality and to design more effective ventilation systems to suitable contaminant dilution.

References

[1] R. Van Gaever, V.A. Jacobs, M. Diltoer, L. Peeters, S. Vanlanduit, Thermal comfort of the surgical staff in the operating room, Build. Environ. 81 (2014) 37–41.
[2] W. Wythe, Cleanroom Technology, Fundamentals and Design, Testing and Operation, 2nd Edition, 2010, John Wiley, 2016.
[3] B. Zhao, Numerical study of particle deposition in two differently ventilated rooms, Indoor Built Environ. 13 (2004) 443–451.
[4] Z. Zhang, Q. Chen, Comparison of the Eulerian and Lagrangian methods for predicting particle transport in enclosed spaces, Atmos. Environ. 41 (2007) 5236–5248.
[5] H. Lee, H.B. Awbi, Effect of internal partitioning on indoor air quality of rooms with mixing ventilation—basic study, Build. Environ. 39 (2004) 127–141.
[6] K. Zhong, X. Yang, Y. Kang, Effects of ventilation strategies and source locations on indoor particle deposition, Build. Environ. 45 (2010) 655–662.
[7] C. Méndez, J.F. San José, J.M. Villafruela, F. Castro, Optimization of a hospital room by means of CFD for more efficient ventilation, Energy Build. 40 (2008) 849–854.
[8] Q. Chen, Z. Jiang, A. Moser, Control of airborne particle concentration and draught risk in an operating room, Indoor Air 2 (1992) 154–167.
[9] I.-P. Chung, D. Dunn-Rankin, Using numerical simulation to predict ventilation efficiency in a model room, Energy Build. 28 (1998) 43–50.
[10] W. Liu, Z. Lian, Y. Yao, Optimization on indoor air diffusion of floor-standing type room air-conditioners, Energy Build. 40 (2008) 59–70.
[11] B. Zhao, Y. Zhang, X. Li, X. Yang, D. Huang, Comparison of indoor aerosol particle concentration and deposition in different ventilated rooms by numerical method, Build. Environ. 39 (2004) 1–8.
[12] S. Sadrizadeh, S. Holmberg, A numerical investigation of vertical and horizontal laminar airflow ventilation in an operating room, J. Infect. Public Health 82 (2014) 517–525.
[13] B.E. Launder, D.B. Spalding, The numerical computation of turbulent flows, Comput. Methods Appl. Mech. Eng 3 (1974) 269–289.
[14] M.H. Saidi, B. Sajadi, G.R. Molaeimanesh, The effect of source motion on contaminant distribution in the cleanrooms, Energy Build. 43 (2011) 966–970.
[15] Q. Chen, Comparison of different k-epsilon models for indoor air flow computations, Numer. Heat Transfer Part B: Fundam. 28 (1995) 353–369.
[16] V. Yakhot, S.A. Orszag, S. Thangam, T.B. Gatski, C.G. Speziale, Development of turbulence models for shear flows by a double expansion technique, Phys. Fluids A: Fluid Dyn. 4 (1992) 1510.
[17] ANSYS Fluent 12.0 user's guide, Ansys Inc, (2009).
[18] Z. Zhang, Q. Chen, Experimental measurements and numerical simulations of particle transport and distribution in ventilated rooms, Atmos. Environ. 40 (2006) 3396–3408.
[19] B. Zhao, C. Yang, X. Yang, S. Liu, Particle dispersion and deposition in ventilated rooms: testing and evaluation of different Eulerian and Lagrangian models, Build. Environ. 43 (2008) 388–397.
[20] A.C.K. Lai, W.W. Nazaroff, Modeling indoor particle deposition from turbulent flow onto smooth surfaces, J. Aerosol Sci. 31 (2000) 463–476.
[21] S.V. Patankar, Numerical Heat Transfer and Fluid Flow, Hemisphere, Washington DC, 1980.
[22] ANSYS ICEM CFD, Ansys Inc (2012).
[23] Ansys Fluent 15.0, Ansys Inc (2013).
[24] F. Chen, S.C.M. Yu, A.C.K. Lai, Modeling particle distribution and deposition in indoor environments with a new drift–flux model, Atmos. Environ. 40 (2006) 357–367.